J. Fluid Mech. (2006), *vol.* 561, *pp.* 465–475.
doi:10.1017/S0022112006000966 Printed in the United Kingdom

Compressible exact solutions for one-dimensional laser ablation fronts

By O. LE MÉTAYER[1,2] AND R. SAUREL[1,2,3]

[1]IUSTI, UMR CNRS 6595, Université Aix-Marseille I, Technopôle de Château Gombert, 5 Rue E. Fermi, 13453 Marseille Cedex 13, France

[2]Projet SMASH, INRIA, 2004 route des Lucioles, 06902 Sophia Antipolis, France

[3]Institut Universitaire de France, 2004 route des Lucioles, 06902 Sophia Antipolis, France
Olivier.Lemetayer@polytech.univ-mrs.fr; Richard.Saurel@polytech.univ-mrs.fr

(Received 8 February 2006 and in revised form 11 April 2006)

When a laser beam of high intensity interacts with a dense material, an ablation front appears in the high-temperature plasma resulting from the interaction. Such a front can be used to accelerate and compress the dense material. The dynamics of the ablation front is strongly coupled to that of the absorption front where the laser energy is absorbed. The present paper determines analytical solutions of the front internal structure in the fully compressible case.

1. Introduction

This study deals with ablation fronts that appear when a high laser beam flux is used to transform a dense material to a lighter one at high velocity and high temperature. This physical process is often used to accelerate and to compress the dense material. As shown in figure 1, the laser beam is absorbed in a critical surface, named the 'absorption front', where the density is determined by the plasma frequency produced. The stored energy is released in the medium by nonlinear thermal diffusion (Spitzer & Härm 1953) which governs the dynamics of a subsonic front, named the 'ablation front', where a high density gradient is present. Through the ablation front, the dense material transforms into a light and hot plasma moving at high velocity towards the absorption zone. This paper is devoted to the determination of the main flow-variable profiles between the ablation front and the absorption front in a one-dimensional steady compressible flow configuration.

The ablation phenomenon is modelled by the Euler equations with additional terms corresponding to thermal diffusion and energy deposition from the laser beam (Clavin & Masse 2004). This energy is stored in the absorption front characterized by a critical density ρ_c.

The system under study is

$$\left.\begin{aligned} &\frac{\partial \rho}{\partial t} + \frac{\partial (\rho u)}{\partial x} = 0, \\ &\frac{\partial (\rho u)}{\partial t} + \frac{\partial (\rho u^2 + P)}{\partial x} = 0, \\ &\frac{\partial (\rho E)}{\partial t} + \frac{\partial ((\rho E + P)u)}{\partial x} = \frac{\partial}{\partial x}\left(\lambda(T)\frac{\partial T}{\partial x}\right) + I\delta_{\{x=x_c(t)\}}, \end{aligned}\right\} \tag{1}$$

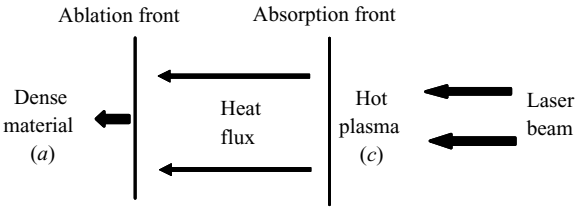

FIGURE 1. Schematic of laser ablation phenomenon.

where ρ, u, P, T represent respectively the density, the material velocity, the pressure and the temperature of the fluid. The total energy is defined as $E = e + u^2/2$ where e is the specific internal energy.

The thermodynamic closure of system (1) is given by the following equations of state (EOS):

$$e(P, \rho) = \frac{P}{(\gamma - 1)\rho}, \tag{2}$$

$$T(P, \rho) = \frac{P}{(\gamma - 1)C_v\rho}, \tag{3}$$

where γ and C_v are constant parameters representing respectively the polytropic coefficient and the heat capacity at constant volume of the fluid. The thermal diffusion corresponds to a contribution of radiation and conduction effects in the plasma. The electronic thermal conductivity obeys the law $\lambda(T) = CT^n$ where C and n are positive constant coefficients (Spitzer & Härm 1953).

Also, in (1) I represents the laser flux intensity and $\delta_{\{x=x_c(t)\}}$ represents the Dirac function associated with the laser deposition at the critical surface x_c characterized by $\rho = \rho_c$. In system (1), this term is written for a laser beam in the opposite direction to the axis x. For the analysis we propose in this paper, it is more convenient to replace the Dirac function with the spatial derivative of the Heavyside function $\delta_{\{x=x_c(t)\}} = \partial H_{\{x>x_c(t)\}}/\partial x$ defined by

$$H_{\{x>x_c(t)\}} = \begin{cases} 1 & \text{if } x > x_c(t) \\ 0 & \text{otherwise.} \end{cases}$$

As a consequence, system (1) can be written in a conservative formulation:

$$\frac{\partial U}{\partial t} + \frac{\partial F}{\partial x} = 0, \tag{4}$$

where $U = (\rho, \rho u, \rho E)^T$ and $F = (\rho u, \rho u^2 + P, (\rho E + P)u + q - IH)^T$ with $q = -\lambda(T)\partial T/\partial x$. The steady solutions of system (4) are obtained by solving the differential system

$$\left.\begin{aligned} \frac{\mathrm{d}\rho u}{\mathrm{d}x} &= 0, \\ \frac{\mathrm{d}\rho u^2 + P}{\mathrm{d}x} &= 0, \\ \frac{\mathrm{d}(\rho E + P)u + q - IH}{\mathrm{d}x} &= 0. \end{aligned}\right\} \tag{5}$$

Hence system (5) is valid in the frame of the ablation front which is considered as a steady front.

The integration of system (5) leads to the following set of equations:

$$\left.\begin{aligned} &m = \rho u = \text{const},\\ &mu + P = \text{const},\\ &m\left(h + \frac{1}{2}\frac{m^2}{\rho^2}\right) + q - IH = \text{const}, \end{aligned}\right\} \tag{6}$$

where $h = e + P/\rho$ is the specific enthalpy of the fluid. System (6) is first studied by neglecting the diffusion term q. This corresponds to the determination of jump relations across a discontinuity separating two constant states without solving its internal structure. These states correspond to those on to each side of the ablation and the absorption fronts. Next, system (6) is studied by considering the diffusion term. The integration of this system allows the determination of the different flow-variable profiles between the two preceding constant states.

2. Study of the jump relations connecting two constant states

Neglecting the diffusion term q, system (6) becomes

$$\left.\begin{aligned} &m = \rho u = \text{const},\\ &mu + P = \text{const},\\ &m\left(h + \frac{1}{2}\frac{m^2}{\rho^2}\right) - IH = \text{const}. \end{aligned}\right\} \tag{7}$$

In the rest of the paper, we will denote by the subscript a the constant state located to the left of the ablation front characterized by knowing $\rho = \rho_a$, $P = P_a$ and $H = H_a = 0$. The only unknown is the material velocity u_a. In the same way, we will denote by the subscript c the constant state located to the right of the absorption front characterized by knowing $H = H_c = 1$ and $\rho = \rho_c$ which corresponds to the critical density.

Then, the algebraic system to solve is the following:

$$\left.\begin{aligned} &m = \rho_a u_a = \rho_c u_c,\\ &mu_a + P_a = mu_c + P_c,\\ &m\left(h_a + \frac{1}{2}\frac{m^2}{\rho_a^2}\right) = m\left(h_c + \frac{1}{2}\frac{m^2}{\rho_c^2}\right) - I, \end{aligned}\right\} \tag{8}$$

where the material velocities u_a, u_c and the pressure P_c are unknown.

The specific enthalpies are given by

$$h_a = \frac{\gamma P_a}{(\gamma - 1)\rho_a} = C_P T_a \quad \text{and} \quad h_c = \frac{\gamma P_c}{(\gamma - 1)\rho_c} = C_P T_c.$$

An interesting limit of system (8), studied in Clavin & Masse (2004), concerns the low-Mach-number quasi-isobaric assumption. In this limit the kinetic energies $\frac{1}{2}m^2/\rho_a^2$ and $\frac{1}{2}m^2/\rho_c^2$ in the total energy equation of system (8) are neglected. Thus, the momentum equation in system (8) is not relevant and only gives an *a posteriori* estimate of the pressure drop across the front.

Under this assumption, the system to consider reduces to

$$m = \rho_a u_a = \rho_c u_c, \quad mh_a = mh_c - I. \tag{9}$$

The temperature T_c is obtained from the equality $P_c = P_a$, that is $T_c = T_a \rho_a / \rho_c$. Then the mass flow rate is directly determined by

$$m = \frac{I}{h_c - h_a} = \frac{I}{C_P(T_c - T_a)} = \frac{I}{C_P T_a (\rho_a/\rho_c - 1)}. \tag{10}$$

The material velocities u_a and u_c are given by the relations $u_a = m/\rho_a$ and $u_c = m/\rho_c$. In the compressible case, the system to solve is

$$\left.\begin{aligned} & m = \rho_a u_a = \rho_c u_c, \\ & \frac{m^2}{\rho_a} + P_a = \frac{m^2}{\rho_c} + P_c, \\ & m\left(h_a + \frac{1}{2}\frac{m^2}{\rho_a^2}\right) = m\left(h_c + \frac{1}{2}\frac{m^2}{\rho_c^2}\right) - I. \end{aligned}\right\} \tag{11}$$

Unlike the quasi-isobaric model, the mass flow rate m cannot be an explicit function of the density ρ_c nor of the temperature T_c. By eliminating the unknown P_c in the energy equation of system (11), a relation between the variables m and ρ_c is obtained:

$$f(m, \rho_c) = \left(\frac{\gamma + 1}{\rho_c} - \frac{\gamma - 1}{\rho_a}\right) m^3 - 2\gamma P_a m + \frac{2(\gamma - 1)I}{(1/\rho_c - 1/\rho_a)} = 0. \tag{12}$$

Since ρ_c is known, the relation (12) is only a function of the mass flow rate m. There always exists a solution corresponding to $m < 0$ and, under some conditions, two solutions corresponding to $m > 0$. The negative solution, which is unphysical, is rejected because the front must be crossed by the matter. In addition, the two positive solutions exist if the following condition is fulfilled:

$$\frac{\rho_a}{\rho_c} \geqslant 1 + \frac{\rho_a((\gamma^2 - 1)I)^2}{2(\gamma + 1)(2/3\gamma P_a)^3}\left(1 + \sqrt{1 + \frac{8(2/3\gamma P_a)^3}{\rho_a((\gamma^2 - 1)I)^2}}\right) = R_\rho^*. \tag{13}$$

This inequality is a compatibility condition between the laser intensity, the thermodynamic state (a) and the critical density ρ_c. If this condition is not fulfilled, the two constant states (a) and (c) cannot be connected and the ablation front does not exist. In particular, for a given thermodynamic state (a) and a given density ratio ρ_a/ρ_c, there exists a maximum value I_{max} for the laser intensity defined as

$$I_{max} = \frac{\left(\frac{2}{3}\gamma P_a\right)^{3/2}(\rho_a/\rho_c - 1)}{(\gamma - 1)\sqrt{\rho_a}\sqrt{(\gamma + 1)\rho_a/\rho_c - (\gamma - 1)}}. \tag{14}$$

This important result is not present in the quasi-isobaric case.

Although an explicit solution for the mass flow rate as a function of ρ_c is not available from (12), an explicit relation linking m and the pressure P_c is readily obtained. By eliminating the density ρ_c in the last two equations of system (11), the following relation is found:

$$m^2 + \frac{(\gamma - 1)\rho_a I}{P_a - P_c} m - \frac{\rho_a}{2}[(\gamma + 1)P_c + (\gamma - 1)P_a] = 0. \tag{15}$$

The solution of (15) corresponding to a negative mass flow rate is rejected. The positive one is

$$m = \frac{(\gamma - 1)\rho_a I}{2(P_a - P_c)}\left(\sqrt{1 + \frac{2(P_a - P_c)^2[(\gamma + 1)P_c + (\gamma - 1)P_a]}{\rho_a((\gamma - 1)I)^2}} - 1\right). \tag{16}$$

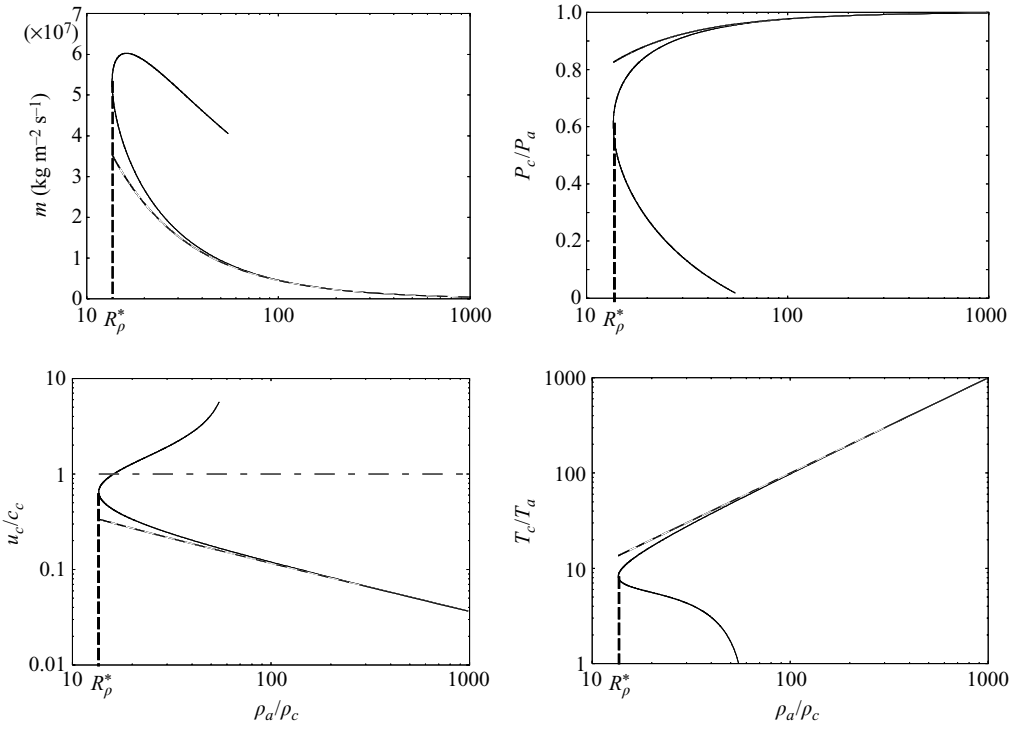

FIGURE 2. Compressible (solid lines) and quasi-isobaric (dashed lines) solutions representing different flow variables as a function of ρ_a/ρ_c.

To reproduce the compressible curves associated with system (11) it is necessary to use an iterative procedure to determine all the flow variables for each value of the ratio ρ_a/ρ_c satisfying relation (13). Such a procedure may be applied by combining relation (16) and the momentum equation of system (11):

$$P_c = P_a + \frac{m^2}{\rho_a}\left(1 - \frac{\rho_a}{\rho_c}\right). \tag{17}$$

Then the material velocities are determined as before with the quasi-isobaric model by the relations $u_a = m/\rho_a$ and $u_c = m/\rho_c$.

In figure 2, the compressible and quasi-isobaric solutions are shown using the following values: $\gamma = 5/3$, $C_P = 5 \times 10^3\,\mathrm{J\,kg^{-1}\,K^{-1}}$, $\rho_a = 10^4\,\mathrm{kg\,m^{-3}}$, $P_a = 9 \times 10^{12}$ Pa and $I = 10^{18}\,\mathrm{W\,m^{-2}}$.

In all the graphs of figure 2, the limit point R^*_ρ given by relation (13) is recovered, showing that no connection between the states (a) and (c) is possible since $\rho_a/\rho_c < R^*_\rho$. In addition another singular point is visible in the graphs related to the mass flow rate and the Mach number: the sonic point. This is characterized by $u = c$ where c is the adiabatic sound speed. At this particular point, the mass flow rate is a maximum, as for the Chapman–Jouguet point in the deflagration branch (Courant & Friedrichs 1948; Le Métayer, Massoni & Saurel 2005). However the study of the front internal structure will show that the supersonic branch of the curves ($M \geqslant 1$) is not physically admissible.

In the next section the profiles of the flow variables connecting the two states (a) and (c) are studied and determined considering the whole system (6).

3. Determination of the internal structure of the front between states (*a*) and (*c*)

In this section we determine the profiles of different flow variables between the ablation front and the absorption front characterized by states (a) and (c). Inside this diffusion zone we always have $H = 0$ because $\rho > \rho_c$. Consequently, system (6) becomes

$$\left.\begin{aligned} &\rho u = \rho_a u_a = m, \\ &\frac{m^2}{\rho} + P = \frac{m^2}{\rho_a} + P_a = Q, \\ &m\left(C_P T + \frac{1}{2}\frac{m^2}{\rho^2}\right) - \lambda \frac{\mathrm{d}T}{\mathrm{d}x} = m\left(C_P T_a + \frac{1}{2}\frac{m^2}{\rho_a^2}\right) = \phi, \end{aligned}\right\} \tag{18}$$

where m, Q and ϕ have been determined thanks to the knowledge of states 'a' and 'c'. The determination of the profiles for the quasi-isobaric model (Clavin & Masse 2004) are first briefly recalled. Then the compressible case is examined.

3.1. *Quasi-isobaric model*

Under this quasi-isobaric assumption, the system to solve is

$$\rho u = \rho_a u_a = m, \quad \rho T = \rho_a T_a, \quad mC_P T - \lambda \frac{\mathrm{d}T}{\mathrm{d}x} = mC_P T_a, \tag{19}$$

where the mass flow rate m is given by relation (10). The unknowns of system (19) are the density $\rho(x)$, the material velocity $u(x)$ and the temperature $T(x)$. The third relation of system (19) provides the temperature profile inside the front. Combining equations of system (19), an ordinary differential equation is obtained:

$$\frac{\mathrm{d}T}{\mathrm{d}x} = \frac{mC_P(T - T_a)}{CT^n}. \tag{20}$$

Once the solution is obtained, the profiles of the density and the material velocity are easily determined by relations $\rho = \rho_a T_a / T$ and $u = m/\rho = mT/\rho_a T_a$.

By denoting

$$\widehat{T} = \frac{T}{T_a} \quad \text{and} \quad \zeta = \frac{mC_P}{CT_a^n} x \overset{\text{def}}{=} \frac{x}{d_a}$$

($d_a = \lambda_a / mC_P$ is the diffusive scale associated with the ablation front), relation (20) becomes

$$\frac{\widehat{T}^n}{(\widehat{T} - 1)} \mathrm{d}\widehat{T} = \mathrm{d}\zeta. \tag{21}$$

Using the relation

$$\frac{\widehat{T}^n}{\widehat{T} - 1} = \frac{1}{\widehat{T} - 1} + \sum_{k=1}^{n} \widehat{T}^{k-1}$$

with an integer $n > 0$, the solution of (21) is

$$\zeta(\widehat{T}) = \zeta_c + \ln \frac{\widehat{T} - 1}{\widehat{T}_c - 1} + \sum_{k=1}^{n} \frac{\left(\widehat{T}^k - \widehat{T}_c^k\right)}{k}. \tag{22}$$

Solutions for particular cases can also be obtained with the help of suitable changes

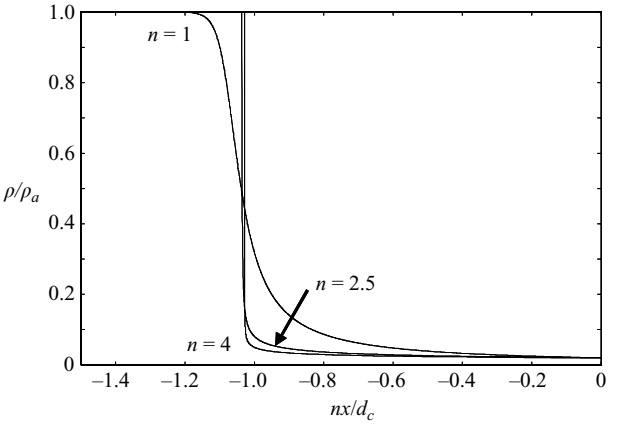

FIGURE 3. Profiles of ρ/ρ_a for different values of the coefficient n in the quasi-isobaric case.

of variables. For example, with $n = 5/2$, the solution is

$$\zeta(\widehat{T}) = \zeta_c + \ln\frac{\widehat{T}^{1/2}-1}{\widehat{T}^{1/2}+1} - \ln\frac{\widehat{T}_c^{1/2}-1}{\widehat{T}_c^{1/2}+1} + 2\big(\widehat{T}^{1/2}-\widehat{T}_c^{1/2}\big) + \tfrac{2}{3}\big(\widehat{T}^{3/2}-\widehat{T}_c^{3/2}\big) + \tfrac{2}{5}\big(\widehat{T}^{5/2}-\widehat{T}_c^{5/2}\big). \quad (23)$$

Obviously, $\widehat{T}$ cannot be expressed as a function of ζ because the preceding relations are not easily invertible. Nevertheless, we can represent the curves $\widehat{T}(\zeta)$ or more exactly the dimensionless curves as a function of nx/d_c where $d_c = \lambda_c/mC_P$ is the diffusive scale associated with the absorption front. This scaling process is used to compare different curves obtained with various values of the coefficient n in a common scale with the same ratio ρ_a/ρ_c. For example, with $\rho_a/\rho_c = 50$, the profile ρ/ρ_a is represented in figure 3 for the values $n = 1$, $n = 5/2$ and $n = 4$ with the origin $\zeta_c = 0$. The values associated with the thermodynamic state (a) and the laser intensity are those given in § 2. In this figure, we can see that the profile ρ/ρ_a steepens as the coefficient n increases, justifying the term 'ablation front'.

3.2. *Compressible case*

In the compressible case, the system to study is

$$\left.\begin{aligned} &\rho u = \rho_a u_a = \rho_c u_c = m,\\ &\frac{m^2}{\rho} + P = \frac{m^2}{\rho_a} + P_a = \frac{m^2}{\rho_c} + P_c = Q,\\ &m\left(C_P T + \frac{1}{2}\frac{m^2}{\rho^2}\right) - \lambda\frac{\mathrm{d}T}{\mathrm{d}x} = m\left(C_P T_a + \frac{1}{2}\frac{m^2}{\rho_a^2}\right) = m\left(C_P T_c + \frac{1}{2}\frac{m^2}{\rho_c^2}\right) - I = \phi, \end{aligned}\right\} \quad (24)$$

where m, Q and ϕ have been computed by relations (16) and (17). The unknowns of system (24) are the density $\rho(x)$, the material velocity $u(x)$, the pressure $P(x)$ and the temperature $T(x)$. To obtain an ordinary differential equation for the temperature T as in the quasi-isobaric case, the density ρ, present in the energy equation of system (24), must be expressed as a function of the temperature T.

By using the momentum equation of system (24) and the EOS $P = (\gamma - 1)\rho C_v T$, an explicit relation between the temperature and the density may be found:

$$T = \frac{1}{(\gamma - 1)C_v \rho}\left(Q - \frac{m^2}{\rho}\right). \tag{25}$$

Before inverting relation (25) to obtain the density ρ as a function of the temperature T, this relation should be analysed, as some important results related to the admissible values of flow variables in state (c) and inside the front internal structure may be deduced. In particular the subsonic character of the flow may be demonstrated.

Subsonic character of the flow inside the front internal structure

By dividing relation (25) by the critical temperature T_c, we obtain:

$$\frac{T}{T_c} = \frac{1}{\mathscr{C}_c^2}\left(\frac{Q}{\rho} - \frac{m^2}{\rho^2}\right) \tag{26}$$

where $\mathscr{C}$ is the isothermal speed of sound defined by $\mathscr{C}^2 = (\partial P/\partial \rho)_T = (\gamma - 1)C_v T$. On using relations $m = \rho_c u_c$ and $Q = \rho_c u_c^2 + P_c = \rho_c(u_c^2 + \mathscr{C}_c^2)$, equation (26) becomes

$$\frac{T}{T_c} = \left(1 + \mathscr{M}_c^2\right)\frac{\rho_c}{\rho} - \mathscr{M}_c^2\left(\frac{\rho_c}{\rho}\right)^2 \tag{27}$$

with the thermal Mach number $\mathscr{M}_c = u_c/\mathscr{C}_c$.

The curve associated with relation (27) has a maximum that depends only on the thermal Mach number at state (c). The values associated with this extremum, represented by superscript $*$, are given by

$$\frac{\rho_c}{\rho^*} = \frac{\mathscr{M}_c^2 + 1}{2\mathscr{M}_c^2} \quad \text{and} \quad \frac{T^*}{T_c} = \frac{\left(\mathscr{M}_c^2 + 1\right)^2}{4\mathscr{M}_c^2}.$$

Now let us assume that the flow is supersonic at the absorption front ($\mathscr{M}_c > 1$). In this case, we have $\rho_c/\rho^* < 1$, which means that this particular point belongs to the internal structure of the front between states (a) and (c) because $\rho_c < \rho^* < \rho_a$. Then, the temperature T reaches the value T^*. Since the flow is assumed to be supersonic ($\mathscr{M}_c > 1$), we have $T^* > T_c$. So the temperature inside the internal structure of the front reaches a value greater than T_c. Consequently, the heat flux $q = -\lambda \mathrm{d}T/\mathrm{d}x$ is positive near the absorption zone.

On the other hand, by using the limits $T \to T_c$ and $\rho \to \rho_c$ in the energy equation of system (24), we get a negative value for the heat flux $q_c = -\lambda_c(\mathrm{d}T/\mathrm{d}x)_c = -I$ in the absorption zone, which is in contradiction with the preceding result. This means that the assumption $\mathscr{M}_c > 1$ is impossible since the ablation front exists. Consequently, the flow must be subsonic at the absorption front ($\mathscr{M}_c \leqslant 1$) and the admissible values of the ratio ρ_a/ρ_c must correspond to the subsonic branch (with respect to the isothermal speed of sound) of the different curves presented in the figure 2. Then no points corresponding to the supersonic branch (with respect to the adiabatic speed of sound) are physically admissible.

Another consequence of this analysis is that the flow must be subsonic (with respect to the isothermal speed of sound) inside the internal structure of the front; the extremum point related to relation (27) divides the associated curve into two parts. One part corresponds to a subsonic branch ($\mathscr{M} < 1$) when $\rho_c/\rho < \rho_c/\rho^*$ and the other corresponds to a supersonic branch ($\mathscr{M} > 1$) when $\rho_c/\rho > \rho_c/\rho^*$. Since the flow is assumed to be subsonic at the absorption front ($\mathscr{M}_c \leqslant 1$), the extremum

point does not belong to the internal structure of the front because $\rho_c/\rho < 1 < \rho_c/\rho^*$. Consequently, the flow inside the front is always subsonic. This important result leads to selection of the appropriate branch ($\mathscr{M} < 1$) when relations (25) and (27) are inverted.

Analytical compressible solutions

With the help of the above analysis, an explicit relation may be obtained from equation (25) expressing the density as a function of the temperature:

$$\frac{m}{\rho} = \frac{Q}{2m} - \left(\left(\frac{Q}{2m} \right)^2 - (\gamma - 1) C_v T \right)^{1/2}. \tag{28}$$

To obtain the profiles of the flow variables between the ablation and absorption fronts, relation (28) is substituted into the energy equation of system (24). We obtain an ordinary differential equation in the temperature, as in the quasi-isobaric case:

$$\frac{C T^n}{m} \frac{\mathrm{d}T}{\mathrm{d}x} = \frac{\gamma + 1}{2} C_v (T - T_a) + \frac{\mathscr{C}_a^2}{4\mathscr{M}_a^2} \left(1 - \mathscr{M}_a^4\right) \left(1 - \sqrt{1 - \frac{4\mathscr{M}_a^2 (\gamma - 1) C_v (T - T_a)}{\mathscr{C}_a^2 \left(1 - \mathscr{M}_a^2\right)^2}} \right) \tag{29}$$

where $\mathscr{C}_a$ and $\mathscr{M}_a$ are respectively the isothermal speed of sound and the Mach number at the ablation front.

By denoting $\widehat{T} = T/T_a$ and $\zeta = (m C_P / C T_a^n) x$, relation (29) becomes

$$\widehat{T}^n \frac{\mathrm{d}\widehat{T}}{\mathrm{d}\zeta} = \frac{\gamma + 1}{2\gamma} (\widehat{T} - 1) + \frac{\gamma - 1}{4\gamma} \frac{\left(1 - \mathscr{M}_a^4\right)}{\mathscr{M}_a^2} \left(1 - \sqrt{1 - \frac{4\mathscr{M}_a^2}{\left(1 - \mathscr{M}_a^2\right)^2} (\widehat{T} - 1)} \right). \tag{30}$$

This ODE can be put into the following form:

$$\frac{\widehat{T}^n}{A\widehat{T} + B - \sqrt{\beta - \alpha \widehat{T}}} \mathrm{d}\widehat{T} = \mathrm{d}\zeta \tag{31}$$

where the coefficients are given by

$$A = \frac{\gamma + 1}{2\gamma}, \quad B = \frac{\gamma - 1}{4\gamma} \frac{\left(1 - \mathscr{M}_a^4\right)}{\mathscr{M}_a^2} - A,$$

$$\alpha = \left(\frac{\gamma - 1}{2\gamma} \right)^2 \frac{\left(1 + \mathscr{M}_a^2\right)^2}{\mathscr{M}_a^2}, \quad \beta = \left(\frac{\gamma}{\gamma - 1} \right)^2 \alpha^2.$$

Now using the change of variable $X = \sqrt{\beta - \alpha \widehat{T}}$, equation (31) becomes

$$\frac{A \alpha^n}{2} \mathrm{d}\zeta = \frac{(\beta - X^2)^n X}{(X + D)(X + E)} \mathrm{d}X \tag{32}$$

with

$$D = \frac{\gamma}{\gamma + 1} \alpha \left(1 + \sqrt{1 + \left(\frac{\gamma + 1}{\gamma - 1} \right)^2 + 2 \frac{\gamma + 1}{\gamma} \frac{B}{\alpha}} \right),$$

$$E = \frac{\gamma}{\gamma + 1} \alpha \left(1 - \sqrt{1 + \left(\frac{\gamma + 1}{\gamma - 1} \right)^2 + 2 \frac{\gamma + 1}{\gamma} \frac{B}{\alpha}} \right).$$

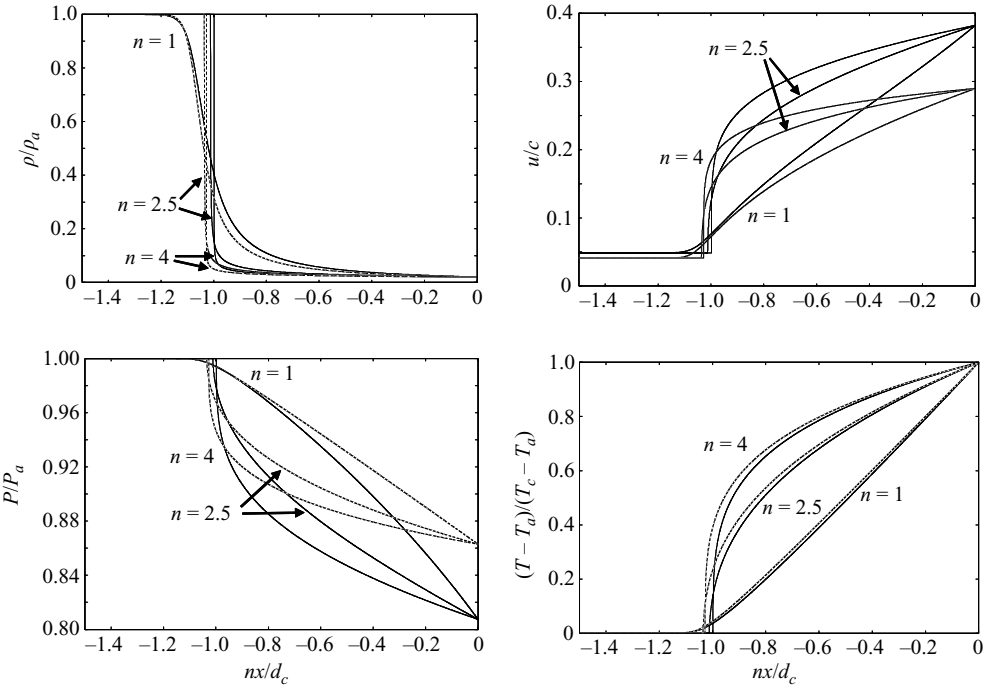

FIGURE 4. Profiles of different flow variables for different values of n in the quasi-isobaric (dashed lines) and the compressible (solid lines) cases.

Solving this ODE is much harder than in the quasi-isobaric case. No simple general formulae are available for an arbitrary value of the coefficient n. Nevertheless, when n is assumed to be an integer, explicit solutions may be found using the following decomposition:

$$\frac{(\beta - X^2)^n X}{(X + D)(X + E)} = \frac{\dfrac{E(\beta - E^2)^n}{X + E} - \dfrac{D(\beta - D^2)^n}{X + D} + \displaystyle\sum_{k=0}^{n} \sum_{l=0}^{2k} \frac{n!}{k!(n-k)!} \beta^{n-k} (-1)^{3k-l} (D^{2k-l} - E^{2k-l}) X^l}{E - D}.$$

Then the integration of relation (32) for an integer $n \geqslant 0$ leads to

$$\frac{(E - D) A \alpha^n}{2} (\zeta - \zeta_c) = E(\beta - E^2)^n \ln\left(\frac{X + E}{X_c + E}\right) - D(\beta - D^2)^n \ln\left(\frac{X + D}{X_c + D}\right) + \sum_{k=0}^{n} \sum_{l=0}^{2k} \frac{n!}{k!(n-k)!} \beta^{n-k} (-1)^{3k-l} (D^{2k-l} - E^{2k-l}) \frac{X^{l+1} - X_c^{l+1}}{l + 1}. \quad (33)$$

In figure 4, the curves corresponding to the solutions of equation (31) and those associated with the quasi-isobaric model are compared for the same ratio $\rho_a/\rho_c = 50$. Again, the values associated with the thermodynamic state (a) and the laser intensity are those given in § 2.

In all the plots of figure 4, as in the quasi-isobaric case, we can see that the profiles of the different flow variables steepen at the ablation front level when the coefficient

n increases. For the same value of $\rho_a/\rho_c = 50$, the mass flow rate $m = \rho_a u_a = \rho_c u_c$ is higher in the compressible case than in the quasi-isobaric case. For this reason, the Mach numbers associated with the states (a) and (c) are greater in the compressible case as we can see in the corresponding graph of figure 4, leading to significant differences at the absorption front level. This result is also visible in the pressure profiles, where the pressure drop is more important in the compressible cases.

We can also see that there are small differences between compressible and quasi-isobaric cases in the density and temperature profiles. The main differences concern the locations of the ablation front and the thickness of the internal structure layer between states (a) and (c).

It is also important to remark that if the value of the ratio ρ_a/ρ_c is less than 50 then the differences between compressible and quasi-isobaric curves are more important because the Mach numbers are much higher in this case, as we can see in figure 2.

4. Conclusion

The ablation front structure of a dense fluid irradiated by a high-energy laser beam has been solved analytically in one space dimension with full compressible effects. Conditions of existence of such fronts have been determined. In particular the subsonic character of the flow at the laser absorption front has been demonstrated leading to conditions for the admissible density jumps at the ablation front. The solutions developed in this paper contain no extra assumptions other than those already involved in the initial flow model. An important aspect of this work is to account for the multidimensional instabilities. In order to carry out such analysis with the same compressible flow model the development of accurate numerical tools is essential. The compressible exact solutions presented herein can be used for the validation and improvement of advanced numerical methods.

The authors are grateful to Professor Clavin for fruitful discussions.

REFERENCES

Clavin, P. & Masse, L. 2004 Instabilities of ablation fronts in inertial confinement fusion: a comparison with flames. *Phys. Plasmas* **11(2)**, 690–705.

Courant, R. & Friedrichs, K. O. 1948 *Supersonic Flow and Shock Waves*. Applied Mathematical Sciences, vol. 21. Springer.

Le Métayer, O., Massoni, J. & Saurel, R. 2005 Modelling evaporation fronts with reactive Riemann solvers. *J. Comput. Phys.* **205**, 567–610.

Spitzer, L. & Härm, R. 1953 Transport phenomena in a completely ionized gas. *Phys. Rev.* **89**, 977.